INTERNATIONAL JOURNAL OF HYDROGEN ENERGY 41 (2016) 2064–2074

Available online at www.sciencedirect.com

ScienceDirect

journal homepage: www.elsevier.com/locate/he

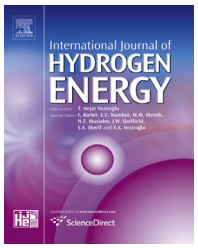

Characterization of the combustion process and cycle-to-cycle variations in a spark ignition engine fuelled with natural gas/hydrogen mixtures

M. Reyes [a,*], F.V. Tinaut [a], A. Melgar [a], A. Pérez [b]

[a] Department of Energy and Fluid Mechanics Engineering, University of Valladolid, Paseo del Cauce 59, E-47011, Valladolid, Spain

[b] CIDAUT Foundation, Parque Tecnológico de Boecillo P.209, E-47151 Boecillo, Valladolid, Spain

ARTICLE INFO

Article history:
Received 17 September 2015
Received in revised form
23 October 2015
Accepted 23 October 2015
Available online 29 November 2015

Keywords:
Cyclic variability
Spark ignition engine
Combustion diagnosis
Hydrogen
Natural gas

ABSTRACT

A study is presented of the influence of using mixtures of natural gas and hydrogen in different fractions (0, 25, 50, 75, 100%) on the combustion velocity and cycle-to-cycle variations in a spark ignition engine. The experimental facility consists of a single-cylinder spark ignition engine. The engine rotational speeds are 1000, 1750 and 2500 rpm. Fuel/air equivalence ratio was kept constant equal to 0.7 during the experiments. A two-zone thermodynamic combustion diagnosis model, based on solving the mass and energy conservation equations, is used to analyze the experimentally obtained pressure combustion chamber in the engine. The two-zone model considers a spherical flame front centred at the spark plug, and solves the intersection of the flame front with the piston, cylinder head and cylinder wall, in order to provide the values of the flame radius corresponding to the burned mass volume and the surfaces for heat to the piston and walls. An automatic procedure based on genetic algorithms is used to determine the optimum parameters needed for combustion diagnosis: Angular positioning and pressure offset of the pressure register, dynamic compression ratio, and heat transfer coefficients. The paper focuses on using the values of the burning velocity computed from the pressure register and especially on the analysis of the cycle to cycle variation in the natural gas/hydrogen fuelled engine, quantified through the standard deviation and the coefficient of variation of the burning speed. Increasing the hydrogen content in the mixture with natural gas increases its burning velocity. This effect is linear with hydrogen fraction, except for very high values of the fraction, when the effect of hydrogen dominates combustion. Additionally, and of practical importance, increasing the hydrogen fraction reduces the relative dispersion of combustion. This effect of hydrogen addition on reducing combustion variability is evident from 25% hydrogen content.

* *Corresponding author.*
E-mail address: miriam.reyes@eii.uva.es (M. Reyes).

http://dx.doi.org/10.1016/j.ijhydene.2015.10.082

Introduction

Due to the increasing interest in energy shortage and environmental protection, much effort has been focused on the use of alternative fuels in internal combustion engines (ICE). Alternative fuels are clean, compared to fuels derived from petroleum. Natural gas (NG) is considered to be a possible alternative fuel due to its properties and higher octane number. NG is a mixture of diverse gases where methane is its major constituent (75–98% of methane; 0.5–13% of ethane; and 0–2.6% of propane [1]). NG combustion causes less emissions than conventional fuels due to the less complex chemical structure of NG and the absence of evaporation phase of the fuel [2]. NG has the capability to completely mix with air eliminating regions with local rich mixture, thus reducing CO emissions. Also, NG produces less CO_2 emissions than gasoline for the same power output, due to its higher hydrogen to carbon ratio [3]. The high octane number of NG (between 120 and 130) represents an elevated anti-knocking potential [4], allowing a spark ignition engine to be operated with a higher compression ratio than by gasoline, so higher thermal efficiency and lower fuel consumption are obtained. Additionally lean mixtures can be stably burned in engines, contributing to a further reduction of CO and HC emissions and an increase in thermal efficiency.

However, NG has a slow burning velocity, compared to other liquid hydrocarbons. Laminar burning velocity is an important property of the combustion process of any fuel/air mixture because fuels with higher burning velocities can improve engine performance [5]. The lower burning velocity in an NG engine requires advancing the spark timing as compared to the gasoline engine, in order to centre the combustion process and optimize indicated efficiency. Additionally the heating value per unit volume of a gaseous fuel–air mixture is smaller than that of a liquid fuel. However, the heating value of the stoichiometric mixture is not so different which is represented by the Engine Fuel Quality (EFQ) defined in Ref. [5].

To increase the burning velocity, it is possible to mix the NG with a fuel with a higher burning velocity, as can be hydrogen [6]. Hydrogen is an attractive fuel due to the variety of methods to produce it [7] and the variety of methods to produce energy from hydrogen (ICE, gas turbines, fuel cells). Some researchers [8,9], have mixed hydrogen with NG or gasoline to increase the burning velocity and then improve the combustion process. The laminar burning velocity of stoichiometric hydrogen-air mixtures is much higher than that of methane (around six or seven times higher at 350 K) [10–13]. Another important thing to consider is that the heating value per unit volume of a NG–hydrogen–air mixture is almost independent of the relative NG/hydrogen ratio [14].

The burning velocity of NG–hydrogen mixtures varying from 0 to 100% have been obtained at different conditions of temperature and pressure. For example, Huang et al. [15] studied the laminar flame characteristics of NG–hydrogen mixtures at normal temperature and pressure, showing that laminar burning velocities increase substantially with the increment of the percentage of hydrogen in the mixture. Also Huang et al. [16,17] studied the combustion characteristics, heat release, engine performance and emissions of a SI engine fuelled with NG–hydrogen mixtures Hu et al. [18] developed an experimental and numerical study of lean mixtures of NG–hydrogen at elevated temperatures and pressures over a wide range of hydrogen percentages in the mixture, showing an increment in the un-stretched laminar burning velocity with the hydrogen fraction and initial temperature. In other works, they studied the combustion characteristics of a SI engine fuelled with NG-Hydrogen and EGR [19,20].

Cycle to cycle variations in spark ignition engines fuelled with NG, hydrogen and mixtures of NG and hydrogen have been extensively studied [21–26], and also in engines fuelled with methanol [27] and ethanol [28] fuels. Sun et al. [25] studied the cyclic variations of an ICE fuelled with hydrogen. They investigated the effect of varying the fuel/air equivalence ratio, the rotational engine speed and the ignition advance angle on the cyclic variations, expressed by the coefficient of variation of the indicated mean effective pressure (COV_{IMEP}). Their results showed a reduction on the cyclic variations with the increment of the fuel/air equivalence ratio, because combustion rate increases with rich mixtures, resulting in a rapid combustion and improving combustion stability. Sen et al. [24] investigated the effect of the exhaust gas recirculation (EGR) on the cycle-to-cycle variations in a NG spark ignition engine, showing that as the percentage of EGR was increased, more persistent low frequency variations tended to develop. Wang et al. [26] studied the effect of hydrogen addition on cycle-by-cycle variations of the natural gas engine. Their results showed that the peak cylinder pressure, the maximum rate of pressure rise and the indicated mean effective pressure increased and their corresponding cycle-by-cycle variations decreased with the increase of hydrogen fraction at lean mixture operation. Huang et al. [21] analyzed the cycle-by-cycle variations in a spark ignition engine fuelled with natural gas–hydrogen blends combined with EGR. Ma et al. [22] conducted a work to investigate the effects of hydrogen addition on the combustion behaviour and cycle-by-cycle variations in a turbocharged lean burn natural gas spark ignition engine. They found that hydrogen addition contributes to reducing the duration of flame development, which has highly positive effects on reducing cycle-by-cycle variations. Reyes et al. [23] characterized mixtures of natural gas and hydrogen in a single-cylinder spark ignition engine by means of a zero dimensional thermodynamic model.

In the work developed by Tinaut et al. [27] different mixtures of NG and hydrogen have been used as fuels to analyze the effect of the addition of hydrogen on the CO and NO emissions, the optimal ignition timing and performance of an ICE.

The experimental study of the combustion process in internal combustion engines through analysis of the combustion chamber pressure is frequently used to accurately know the evolution of the relevant thermodynamic variables, such as temperature, heat release, turbulent combustion speed, etc. These studies are usually focused on the improvement of thermal efficiency and reduction of pollutant emissions. Depending on the aim of the combustion study, different kinds or categories of models can be proposed: zero-dimensional models, two-zone diagnostic models, multi-zone models, etc. [28–30], all of them make a thermodynamic analysis of the pressure inside the cylinder during the combustion process. The outputs of the models are expressed

as characteristic variables such as the Mass Fraction Burned (MFB) and the burning velocity, among others.

However, the methodology based on analyzing the experimental in–cylinder pressure suffers from the uncertainties associated to the measurement: pressure offset, angular positioning, heat transfer effects. These parameters have different values for each particular engine cycle. This makes difficult their adjustment, which is a need in order to obtain an exact diagnosis of the combustion process. In the present work, an adjusting method based on a genetic algorithm strategy is used in order to ensure an objective and optimal adjustment. Genetic algorithms were first introduced by Holland [31]. These algorithms are generally used to solve optimization problems and have been widely used [32,33], confirming to be a potent tool to solve complex problems.

The authors have developed a two-zone diagnostic model, with temperature dependent thermodynamic properties and consideration of heat losses, to perform an analysis of engine combustion pressure. In combination with a procedure based on genetic algorithms, the diagnostic tool can eliminate the subjectivity (i.e. bias errors) introduced by the operator in obtaining results and to increase the analysis capability to using hundred of engine pressure cycles. In the work, six series of 830 consecutive engine pressure cycles have been analyzed, obtaining the combustion diagnosis of each cycle.

The principal objective of this work is to obtain an estimation of the influence of the percentage of hydrogen in the fuel mixture of a single-cylinder spark ignition engine on the combustion velocity and cycle-to-cycle variations. Mixtures of natural gas and hydrogen in five different proportions (0, 25, 75, 100% of hydrogen in volume), with different engine speeds (1000 rpm, 1750 rpm and 2500 rpm) and a fuel/air equivalence ratio of 0.7 are used as fuel in the engine studied.

Methodology

Experimental apparatus and procedure

The tests were performed in a single-cylinder, four-stroke, air cooled MINSEL M380 engine. This engine was originally designed to be a compression ignition engine, with a flat cylinder head and a bowl-in-piston combustion chamber. A number of changes were made to transform it into a spark ignition engine. The original injector was substituted by a spark plug and a modification in the piston was carried out in order to transform the combustion chamber and to reduce the original compression ratio. The dimensions of the cylinder are: 80 mm bore, 75 mm stroke, with an 11.4 compression ratio.

This engine was coupled to a 5.5 kW LEROY SOMER asynchronous machine that was used for motoring and braking, see Fig. 1. The engine was instrumented for the measurement of mean engine performance variables to determine when it is stabilized, such as intake and exhaust pressures, and intake, exhaust, cylinder head and oil temperatures. When the engine is stabilized at a certain operating point, the instantaneous pressure in the combustion chamber is registered and stored in the digital oscilloscope. IMEP at each operating point is then calculated from the instantaneous pressure plot.

The experiments have been carried out at 0.7 fuel/air equivalence ratio, for three different engine rotational speeds: 1000 rpm, 1750 rpm and 2500 rpm, to discern the effect of the engine rotational speed on the cyclic dispersion. For each engine rotational speed the percentage of hydrogen in the natural gas was increased from 0, 25, 50, 75 and 100%. The composition of natural gas is showed in Table 1.

Cylinder pressure measurement

In the experimental setup, the pressure inside the cylinder was measured by using a piezo-electric sensor AVL GU21D (maximum calibration error of 0.06%). This sensor was connected to a KISTLER 5018A1000 charge amplifier (maximum calibration error of 0.3%). The output signal of the charge amplifier was recorded on a Yokogawa DL750 Scopecorder (16 bits AD converter). The estimated error of the pressure acquisition is 0.36% over the measuring range. The crankshaft angle was measured using a free end AVL 360C.03 angular encoder. This encoder has 600 marks per revolution: i.e. a 0.6degrees resolution and also a single pulse per revolution signal. In order to synchronize the pressure signal with the crankshaft angle, the option of an external clock was activated

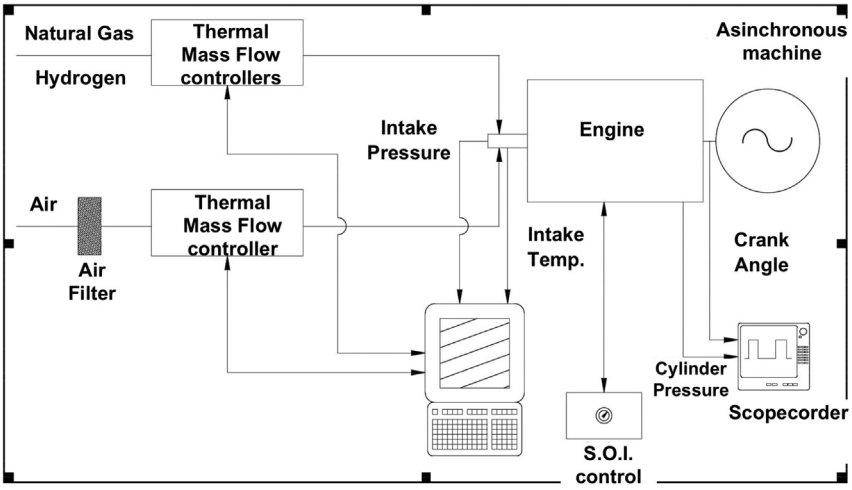

Fig. 1 – Schematic diagram of the engine setup.

Table 1 – Natural gas composition.

Natural gas (Composition)	
Components	Content
C_6	0.002%
Propane	1.040%
Iso-Buthane	0.091%
N-Buthane	0.097%
Iso-Pentane	0.019%
N-Pentane	0.012%
CO_2	1.630%
Ethane	7.840%
N_2	1.043%
Methane	88.226%

in the Scopecorder. In Table 2 are presented the description of the tests carried out.

Mass flow set and measurement

The fuels used during the experiments were natural gas and hydrogen. The inlet mixture of NG, hydrogen and air was established with three BROOKS thermal mass flow controllers. These controllers are equipped with a proportional valve and an actuator. Therefore, the mass flow rate could be measured and controlled at once. A 5853S model was used for the air and a 5851S model was used for the NG and hydrogen. The mixture of the NG, hydrogen and air was formed in the inlet manifold, so the level of premixing was high and almost constant.

Thermodynamic model

MFB is determined from the experimentally obtained pressure in the engine combustion chamber by making use of a two-zone thermodynamic combustion diagnosis model, based on solving the mass and energy conservation equations in two zones. . The model has a quasi-dimensional character, in the sense that it accounts for the flame front position, and solves the energy conservation equation in two zones, not only the apparent heat release. This model considers the separation of the combustion chamber into two-different zones: Burned (denoted with a b subscript) and unburned (denoted with an ub subscript), and the application of the conservation equations, with ideal gas behaviour in each zone. During combustion, the unburned zone converts into burned zone, which starts at the spark ignition electrodes, and the burned zone grows spherically in a concentric way with the combustion chamber wall. Among other variables, the outputs of this model are the temperature of the unburned and burned zones, and the burned mass fraction. From the latter, with the assumption of a spherical flame front, the burning velocity is obtained [34,35].

Table 2 – Tests conditions.

% H2	% NG	Engine speed (rpm)	Ignition timing (crank angle before TDC)
0	100	2500	31.2
25	75	2500	28.8
50	50	2500	24.6
75	25	2500	20.4
100	0	2500	12
0	100	1750	32.4
25	75	1750	28.2
50	50	1750	25.8
75	25	1750	18
100	0	1750	9.6
0	100	1000	30.6
25	75	1000	24.6
50	50	1000	21.6
75	25	1000	16.2
100	0	1000	5.4

More specifically, the two-zone thermodynamic model is based on the following hypotheses:

- The total mass inside the bomb is constant during the combustion process (no leakage).
- Temperature, chemical composition and other intensive properties are represented by their mean values in each zone.
- The pressure at any instant during the combustion is uniform and is the same throughout the chamber, because the engine combustion is considered a deflagration.
- In each zone, the ideal gas equation is used as the thermal state equation.
- The flame front is assumed to be semi-spherical. The change from the unburned to the burned state takes place across the flame front.
- Unburned mixture is assumed to have the constant chemical composition given by the proportion of hydrogen/natural gas and equivalence ratio, while the composition of the burned gases is the equilibrium composition for the corresponding pressure, temperature and equivalence ratio.
- Heat transmission is considered between each zone, burned and unburned, and the walls respectively, but not between both zones. The heat transmission surfaces of each zone are the part of wetted surfaces of the piston, cylinder head and cylinder walls of the burned and unburned zone respectively.

Under these conditions, the main equations of the two-zone thermodynamic model are the following ones:

Energy equations:

$$\text{Unburned zone}: \quad \frac{dU_{ub}}{dt} = \dot{Q}_{ub} + \dot{W}_{ub} - \dot{m}_{ub\to b} h_{ub} \tag{1}$$

$$\text{Burned zone}: \quad \frac{dU_b}{dt} = \dot{Q}_b + \dot{W}_b + \dot{m}_{ub\to b} h_{ub} \tag{2}$$

where the subscripts ub and b refer to the unburned and burned zones respectively, U is the internal energy, t the time, Q the heat loss to the walls, W the work done over each zone due to the volume change, $\dot{m}$ the mass flow rate and h the specific enthalpy.

Mass conservation equations:

$$\dot{m}_{ub} = -\dot{m}_{ub\to b} \tag{3}$$

$$\dot{m}_b = \dot{m}_{ub\to b} \tag{4}$$

Volume restriction:

$$V = V_{ub} + V_b \tag{5}$$

$$\frac{dV_{ub}}{dt} = \frac{dV}{dt} - \frac{dV_b}{dt} \tag{6}$$

where V is the volume of the chamber of combustion, depending on the crank angle, V_{ub} and V_b are the volumes of the unburned and burned zones, which are calculated with a geometrical model explained in the following section.

State equation in each zone:

$$pV_{ub} = m_{ub}R_{ub}T_{ub} \tag{7}$$

$$pV_b = m_bR_bT_b \tag{8}$$

where R is the gas constant particularized for the gas composition of each zone (unburned and burned), p the pressure and T the temperature of each zone.

The internal energies, heat fluxes, work fluxes and enthalpies can be calculated as functions of temperatures, volumes, chemical composition and pressure. The unburned zone composition is constant and known, while the burned zone composition can be obtained with the pressure, the burned zone temperature and the unburned zone composition, by supposing chemical equilibrium. The flame front position or, what it is equivalent, its radius, can be obtained from the geometrical model.

The burning velocity is then calculated as a result from the mass burning rate, the unburned mixture density and the flame front surface, according to the following expression:

$$C_c = \frac{\dot{m}_b}{\rho_{ub}A_f} \tag{9}$$

where C_c is the burning velocity, ρ_{ub} is the density of the unburned mixture and A_f is the flame front surface.

Geometrical model for the flame during combustion process

In Eq. (9) the unburned zone density is obtained from the unburned temperature and the chamber pressure, the combustion rate is a result of the thermodynamic model, and the flame front area is the area of a semi-spherical surface contained inside the volume of the burned zone, but taking into account the instantaneous position of the piston. The radius of the flame front and especially the intersections of the flame front with the piston and the wetted surfaces (piston, cylinder head, and cylinder wall) are calculated by means of a geometrical model, by considering two main cases: firstly when the flame front does not yet touch the piston (and thus is semi-spherical) and secondly when the flame front touches the piston and is the initial semi-sphere is distorted. In the following sections both cases are explained in detail.

Flame front does not touch the piston

In Fig. 2i a schematic picture of the flame front is represented when the first does not yet touch the piston. In this case the flame front area is straightforwardly given by the burned volume V_q with the hypothesis of a semi-spherical flame front of radius R_f.

Flame front intersects the piston

Fig. 2ii represents the case in which the flame front intersects the piston, where Xp is the piston distance with respect to the cylinder head, R_0 is the radius of the cylinder defined by the flame front and piston intersection (see Fig. 2ii), r is the generic distance to the axis of the piston and y(r) is the depth of the piston bowl relative to the piston upper face for each r.

Then, the burned volume is the addition of three parts:

$$V_q = V_1 + V_2 + V_3 \tag{10}$$

where:

$$V_1 = \int_0^R 2\pi \cdot r \cdot y(r)dr \tag{11}$$

This integral can be solved by discretizing it in N points with the piston bowl depth as a function of the radius R_p:

$$V_1 = \sum_{i=0}^{N} 2\pi r_i y_i \frac{R_p}{N-1} \tag{12}$$

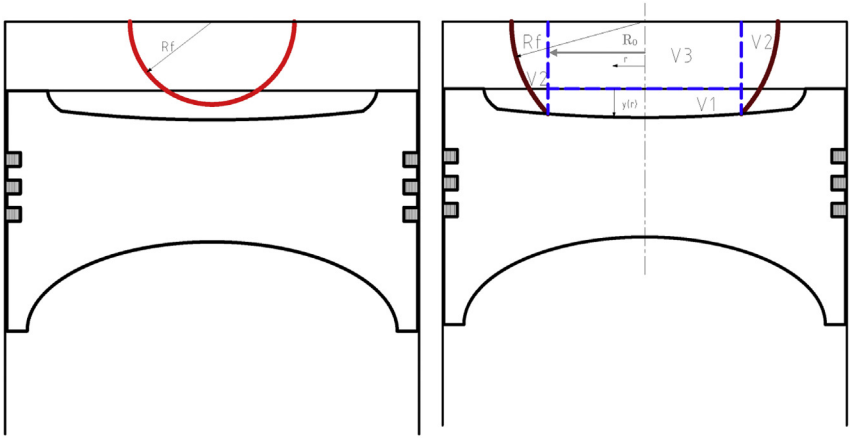

(i) (ii)

Fig. 2 – Geometrical configuration: (i) the flame front does not touch the piston, and (ii) flame front intersection with the piston.

V_2 is calculated as the volume of a semi-sphere with radius R, minus the volume of a cylinder of height Y_0 and radius R_0, and minus the volume of a spherical cap with a radius R_0 and height l_0, see Fig. 2ii.

$$V_2 = \frac{2}{3}\pi R^3 - \int_{l_0}^{R} \pi S(l)^2 dl - \pi R_0^2 l_0 = \frac{2}{3}\pi l_0^3 \quad (13)$$

V_3 is calculated as the volume of a cylinder with radius R_0 and height X_p.

$$V_3 = 2\pi R_0^2 X_p \quad (14)$$

At any instant, V_1, V_2 and V_3 are calculated by iterating the value of the radius R until their summation reaches the value of the burned volume $V_q = V_1 + V_2 + V_3$. Then the flame front radius and area take the following values:

$$R_f = \sqrt{(Y_0 + X_p)^2 + R_0^2} \quad (15)$$

$$A_f = 2\pi R_f^2 \quad (16)$$

Genetic algorithm

With the purpose of processing the pressure data with the thermodynamic model, the authors use an application of genetic algorithms to solve the positioning of the pressure diagram and to adjust the rest of parameters of the engine that are difficult to know precisely.

Genetic algorithms are based on Darwin's Theory of Evolution: the best adapted individuals are selected to survive and to be the progenitors of the next generation. Thus by this selection, the best genetic combination is transmitted to the following generation of individuals. This procedure, repeated numerous generations, ends with a new, better-adapted individual. This method is programmed to obtain the most precise combustion diagnosis for each engine cycle. This ensures that the best determination of MFB is obtained for each cycle in an objective manner.

Any genetic algorithm used to solve an optimization problem has several concepts in common: individual, codification, fitness function, selection and genetic operators. The criterion to select the best adapted individuals is applied by using the fitness function Z (applied to the MFB calculated with the diagnostic model for each individual codification).

Each individual is characterized by its codification. The parameters that must be adjusted by the algorithm are: Angular position, pressure offset, compression ratio and a multiplier of the heat transfer coefficient, calculated by using Woschni's correlation [36]. The evaluation criterion to select the better adapted individuals is a fitness function which is applied to the result of the diagnostic model, run with the parameters of each individual. The general objective of the optimization procedure is to reduce the error of the fitness function, for each of the cycles registered, both for motored conditions (mass fraction burned zero, 11 cycles) and combustion conditions (mass fraction burned different from zero, 830 cycles in each operating condition). Detailed information of the crossover function and the Z function can be found in Reyes et al. [23] where a full description of the used genetic algorithm is presented with supplementary information.

Results and discussion

Analysis of cyclic variations

In this section results of the burning velocity obtained with the thermodynamic model are analyzed for different engine speeds (1000 rpm, 1750 rpm and 2500 rpm) and fraction of hydrogen in the mixture of hydrogen–NG (0, 25, 50, 75 and 100) to study the influence of the fraction of hydrogen in the fuel mixture. The burning velocity C_c that is presented is the result of ensemble averaging the values of 830 combustion cycles. This ensemble averaging process is done by considering all the values of C_c of the individual cycles that have the same mass fraction burned (which is slightly different from ensemble averaging for the same angular position). In addition, the standard deviation (Sigma) and the coefficient of variation (COV = C_c/Sigma) are also presented and considered for the analysis.

Traditionally these three variables are plotted as functions of time. However, since combustion duration changes a lot from one operating condition to other, due to the strong differences of the laminar burning velocity of hydrogen and natural gas, plus the effect of engine rpm, it would be very difficult a direct comparison of results. For that reason, C_c, Sigma and COV are represented versus the mass fraction burned (MFB), which always varies from 0 to 1. In Fig. 3, an example of the burning velocity C_c of 50 individual cycles plotted versus the mass fraction burned is presented. It can be seen that the cyclic dispersion in combustion pressure is reproduced in the burning velocity. The average value of burning velocity is made by ensemble-averaging the values of C_c for each value of MFB (instead of crank angle-averaging for

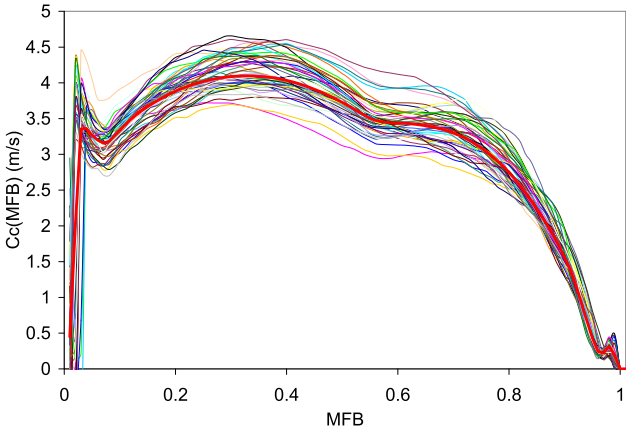

Fig. 3 – Plot of burning velocity C_c of 50 combustion cycles versus the mass fraction burned MFB and comparison with the ensemble averaged burning velocity (in thick, red dots) for 1000 rpm and 25% of hydrogen in natural gas. (For interpretation of the references to color in this figure legend, the reader is referred to the web version of this article.)

each value of crank angle). The ensemble averaged value of C_c is also plotted for comparison (in thick, red symbols). The analysis and plots of the rest of the paper refers to this ensemble averaged burning velocity, its standard deviation and its coefficient of variation.

In Fig. 4 the ensemble averaged burning velocity C_c is represented versus the mass fraction burned (MFB) for the five different mixtures of hydrogen and natural gas. As the engine speed grows (from below to above) the burning velocity increases, as can be expected due to the turbulent nature of combustion flow. In all the three graphs it can be seen that the burning velocity increases as the fraction of hydrogen increases in the mixtures, independently of the engine speed.

However, the lines corresponding to 100% hydrogen are qualitatively different, since they are distinctly separated from the other, showing what it is known as "hydrogen-dominated combustion".

In Fig. 5 the standard deviation Sigma of the burning velocity is presented in the same conditions. This Sigma is an estimator of the cyclic variability, complementing other estimators such as the standard deviation of maximum pressure, indicated mean effective pressure or combustion duration [37].

As can be seen in the three plots of Fig. 5, there is a general effect of engine speed on the values of Sigma of C_c, which increases as engine rpm increases (as the value of C_c itself makes in Fig. 4).

This is again a consequence of the turbulence of the engine in–cylinder flow, with a turbulent intensity that scales with engine speed, increasing not only the average value (C_c) but also its variability (Sigma). One important thing to point

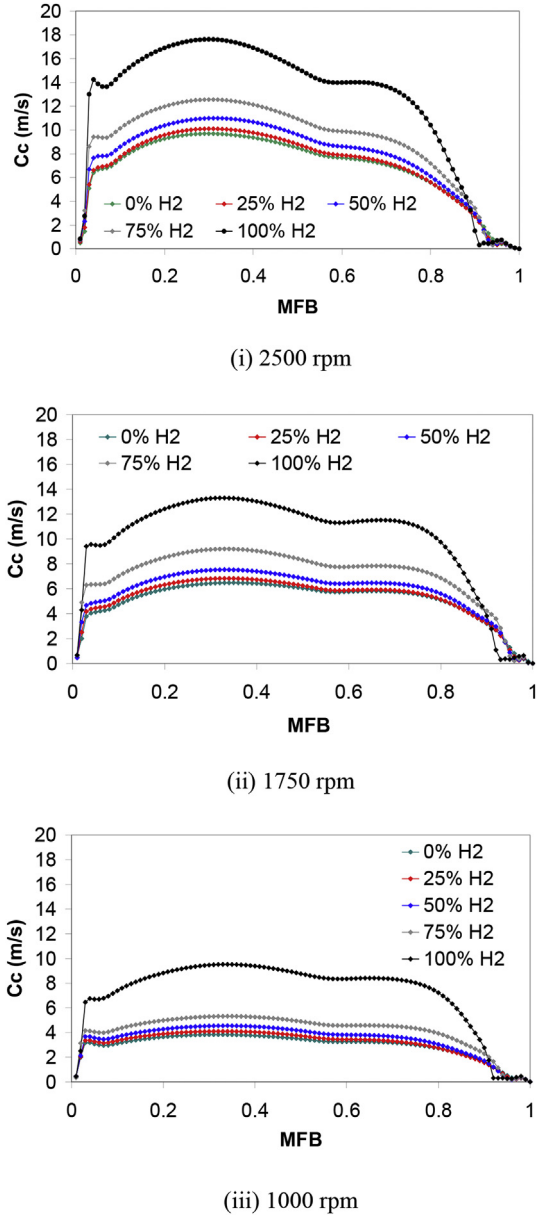

Fig. 4 – Averaged burning velocity C_c versus the mass fraction burned MFB for different engine speeds and different fractions of hydrogen/natural gas.

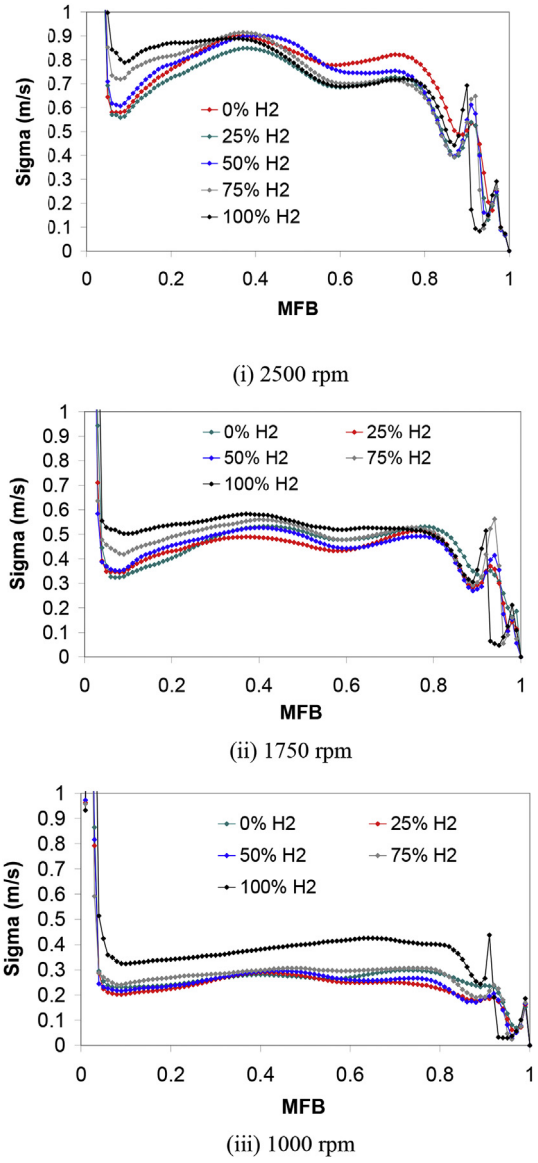

Fig. 5 – Standard deviation Sigma of the burning velocity versus the mass fraction burned MFB for different engine speeds and different mixtures of hydrogen/natural gas.

out is that the variability of the burning velocity (Fig. 5) is much less dependent on the fraction of hydrogen in the fuel mixture, than the burning velocity itself (Fig. 4), with perhaps the exception of pure hydrogen at 1000 rpm. For 1750 and 2500 rpm, it can be seen that the values of Sigma are similar in all the cases, with small differences when the hydrogen fraction changes. This suggests that the combustion process is mainly dominated by the turbulence inside the combustion chamber due to the admission and compression processes.

However, in the case of pure hydrogen at 1000 rpm, the values of Sigma are clearly higher than for the other fractions. This is probably a consequence of the very high transport properties of hydrogen, which at low levels of flow turbulence (i.e. low rpm) are more relevant that the enhanced transport effects due to turbulence.

In Fig. 6 the values of the coefficient of variation of the burning velocity (COV), calculated as the ratio of the standard deviation Sigma and the averaged value of the burning velocity C_c, are plotted versus MFB for the three engine rpm and hydrogen fractions.

This COV represents a measurement of the dispersion of combustion speed relative to the average value. Since in addition the COV is dimensionless, it is usually considered as a better estimator of cyclic dispersion than just the standard deviation of Sigma. As can be seen, in general the values of COV vary much less with engine rpm than the separate values of C_c and Sigma (which have both an increasing trend).

As regard to the trend with hydrogen fraction, the COV shows more distinctly than Sigma the effects of hydrogen contents in the mixture, with the lines in Fig. 6 much more separated than those in Fig. 5. In particular, the values of COV for each value of MFB are ordered in descending values as the hydrogen fraction increases. This is an important conclusion, since it means that increasing the hydrogen content in the mixture with natural gas increases its burning velocity (Fig. 4) and reduces the relative dispersion of combustion (Fig. 6). Moreover, while it is necessary to increase significantly the hydrogen content to have a relevant increase in burning velocity, the effect of hydrogen addition on reducing combustion variability is evident from at least 25%.

The effect on burning velocity of hydrogen fraction is shown in more detail in Fig. 7. In it, several graphs are plotted, with the burning velocity versus the hydrogen fraction for each engine rpm. Since the burning velocity varies along the combustion process (check Fig. 4), particular values of it at relevant values of MFB have been selected to show the trends. In particular, the values of C_c at MFB equal to 0.05, 0.10, 0.25, 0.50 and 0.75 are considered, as representative of the initial, central and final parts of combustion process.

The general trends are similar for all values of engine rpm, with bigger values of C_c as engine rpm increases. However the differences are stronger for 0.25 and 0.50 MFB, since the combustion induced turbulence is not yet strong.

This is in accordance to the fact that the dependence of C_c on rpm is practically the same for 0.05 and 0.10 MFB. On the contrary for 0.75 MFB, the dependence of C_c on rpm is smaller, since combustion rate at that MFB is more influenced by the previous combustion development than by initial flow turbulence.

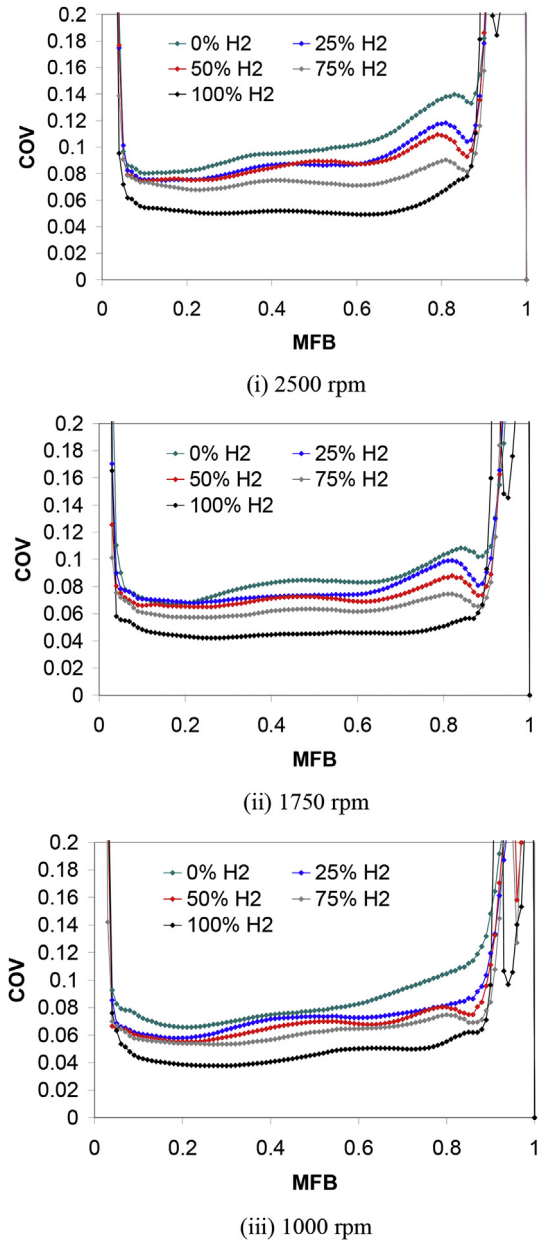

Fig. 6 – Coefficient of variation COV of the burning velocity versus the mass fraction burned for diverse engine speeds and different mixtures of hydrogen/natural gas.

Fig. 8 shows combined results of the burning velocity for the three engine speeds as a function of the hydrogen percentage in the fuel mixture for each MFB value. The tendency of the burning velocity with the percentage of hydrogen, previously observed in Fig. 7, appears clearly in Fig. 8 for the three engine speeds considered.

In this Figure also can be observed a big increment of the burning velocity when the percentage of hydrogen in the mixtures increases from 75% to 100% and appears for all the engine speed and MFB. This increment is more important for low engine speeds (i.e. for 1000 rpm the increase in the burning velocity is between 65 and 85%) and it is obtained for all the considered MFB values. The increment in the

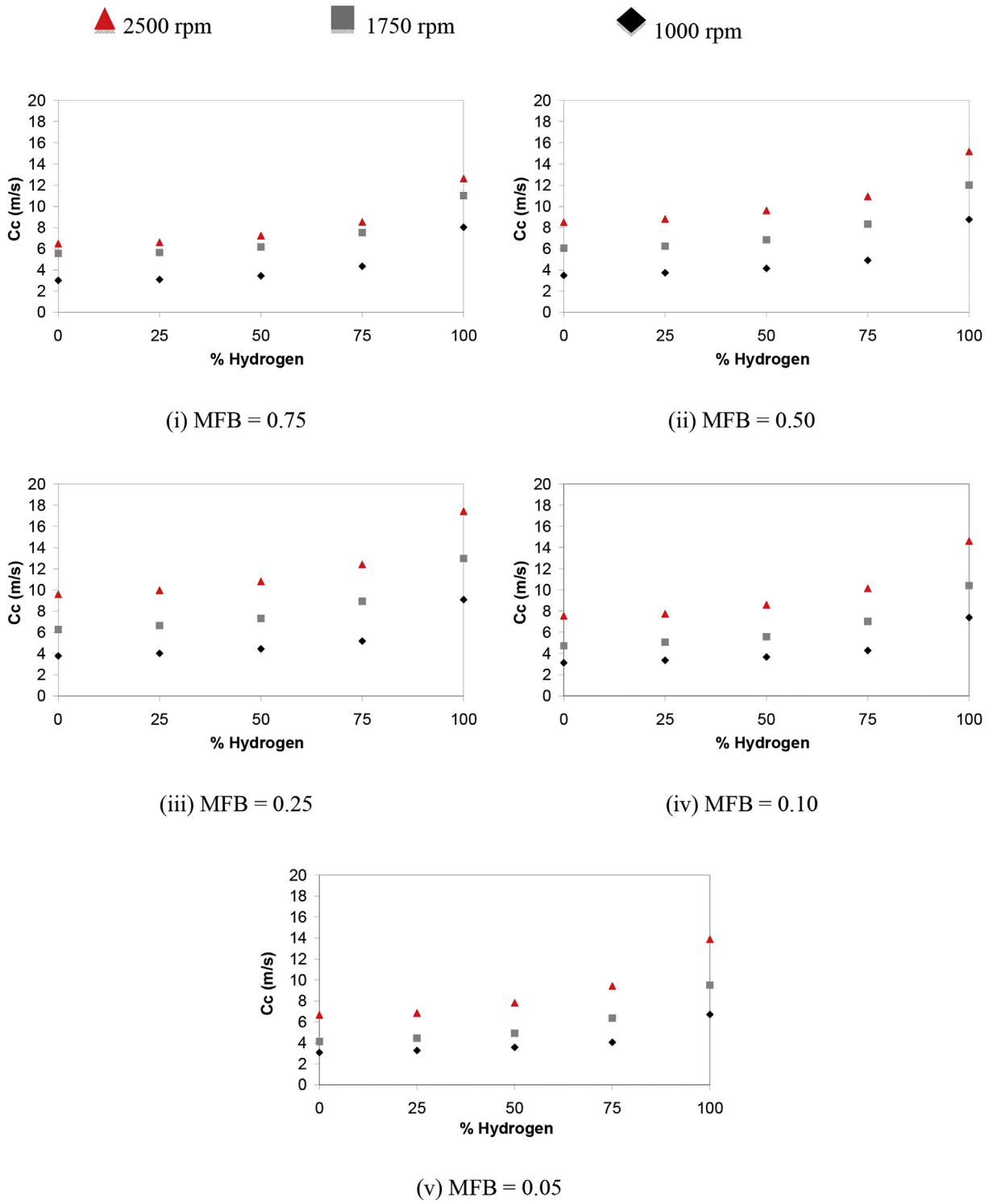

Fig. 7 – Values of ensemble averaged burning velocity C_c versus hydrogen fraction for selected values of mass fraction burned (MFB) at three engine rpm.

burning velocity for other engine rpm is less notable, around 45%, when the percentage of hydrogen in the mixture changes from 75 to 100%. This effect is visible from the early stage of combustion and keeps along all combustion process.

Conclusions

The work presented is based on the use of a two-zone thermodynamic model to analyze combustion pressure in a one-cylinder spark ignition engine fuelled with hydrogen/natural

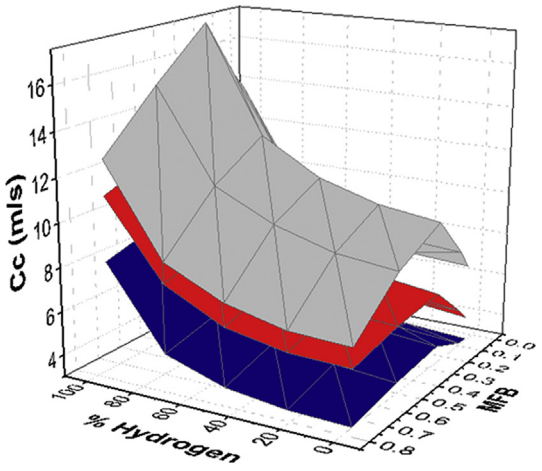

Fig. 8 – Burning velocity versus the percentage of hydrogen in the mixture and the MFB (2500 rpm 1750 rpm 1000 rpm).

gas blends under lean combustion. The geometric character of the model provides a means to relate the combustion rate and the burning velocity. The use of the model is complemented with a procedure based on genetic algorithms to objectively obtain the adjusting experimental values of the pressure plots.

The systematic use of the model on long series of more than 800 combustion cycles (experimental pressure-crank angle registers) allows obtaining quantitative values of the burning velocity (first as a function of crank angle and then of mass fraction burned), the ensemble-averaged value of burning velocity as a function of mass fraction burned, and the associated values of standard deviation and coefficient of variation. The graphical representation of these variables versus the mass fraction burned MFB allows identifying more clearly the trends as engine rpm and hydrogen fraction change.

From the analysis of results performed, the following general trends of the effect of hydrogen addition to natural gas can be reached:

Since the laminar burning velocity of hydrogen is much higher than that of natural gas, increasing the hydrogen content in the mixture with natural gas increases its burning velocity. This effect is more or less linear as hydrogen fraction increases from zero, except for very high values of the fraction, when the effect of hydrogen dominates combustion, even reducing the enhancing effect of flow turbulence. This effect is noticeable from the early phase of combustion (MFB equal to 0.05) and keeps along all combustion process (up to MFB higher than 0.75), for all values of engine rpm. The relative increase of combustion velocity is higher for low engine rpm (about 65% for 1000 rpm, and 45% for 1750 and 2500 rpm).

Additionally, increasing the hydrogen fraction reduces the relative dispersion of combustion, as measured by the coefficient of variation COV. This effect of hydrogen addition on reducing combustion variability appears for all engine rpm and is already evident for 25% hydrogen. Moreover the reduction is more important at the early stage of combustion (between 0.01 and 0.05 MFB).

Acknowledgments

The authors of this work would like to thank the Spanish Ministry of Science and Innovation for the financial support of this research through the ENE 2012-34830 (with FEDER funds) and the Regional Government of Castile and Leon for funding the Excellence Research Group GR203.

Nomenclature

A_f	flame front area, m^2
C_c	burning velocity, m/s
EGR	Exhaust Gas Recirculation
ICE	internal combustion engine
h	specific enthalpy, J/kg
IMEP	indicated mean pressure, Pa
m	total mass, kg
MFB	mass fraction burned, –
MFBR	mass fraction burning rate, 1/° or 1/s
NG	natural gas
p	pressure, Pa
Q	heat loss to the walls, J
R_f	flame front radius
R_j	universal gas constant
t	time, s
T	temperature, K
U	internal energy, J
V	volume, m^3
W	work, J

Greek

α	crank angle, ° or rad
ρ	density, kg/m^3
σ-sigma	standard deviation

Subscripts

b	burned
max	maximum
ub	unburned, fresh

REFERENCES

[1] Naber JD, Siebers DL, Di Julio SS, Westbrook CK. Effects of natural gas composition on ignition delay under diesel conditions. Combust Flame 1994;99:192–200.
[2] El-Sherif AS. Effects of natural gas composition on the nitrogen oxide, flame structure and burning velocity under laminar premixed flame conditions. Fuel 1998;77:1539–47.
[3] Rosen J. Running on methane. Mech Eng 1990;112:66–71.
[4] Das LM, Gulati R, Gupta PK. A comparative evaluation of the performance characteristics of a spark ignition engine using hydrogen and compressed natural gas as alternative fuels. Int J Hydrogen Energy 2000;25:783–93.
[5] Cracknell R, Prakash A, Head R. Influence of laminar burning velocity on performance of gasoline engines. SAE Int; 2012. Sae Paper 2012-01-1742.
[6] Akansu SO, Dulger Z, Kahraman N, Veziroğlu TN. Internal combustion engines fueled by natural gas—hydrogen mixtures. Int J Hydrogen Energy 2004;29:1527–39.

[7] Yilanci A, Dincer I, Ozturk HK. A review on solar-hydrogen/fuel cell hybrid energy systems for stationary applications. Prog Energy Combust Sci 2009;35:231–44.
[8] Ji C, Wang S. Experimental study on combustion and emissions performance of a hybrid hydrogen–gasoline engine at lean burn limits. Int J Hydrogen Energy 2010;35:1453–62.
[9] Ji C, Wang S. Combustion and emissions performance of a hybrid hydrogen–gasoline engine at idle and lean conditions. Int J Hydrogen Energy 2010;35:346–55.
[10] Verhelst S, Wallner T. Hydrogen-fueled internal combustion engines. Prog Energy Combust Sci 2009;35:490–527.
[11] Lafuente A. Methodology for the diagnostic of the laminar burning velocity of fuel gas mixtures from the pressure inside a constant volume combustion bomb. University of Valladolid; 2008.
[12] Gerke U, Steurs K, Rebecchi P, Boulouchos K. Derivation of burning velocities of premixed hydrogen/air flames at engine-relevant conditions using a single-cylinder compression machine with optical access. Int J Hydrogen Energy 2010;35:2566–77.
[13] Kosmadakis GM, Rakopoulos CD, Demuynck J, De Paepe M, Verhelst S. CFD modeling and experimental study of combustion and nitric oxide emissions in hydrogen-fueled spark-ignition engine operating in a very wide range of EGR rates. Int J Hydrogen Energy 2012;37:10917–34.
[14] Wang J, Huang Z, Miao H, Wang X, Jiang D. Study of cyclic variations of direct-injection combustion fueled with natural gas–hydrogen blends using a constant volume vessel. Int J Hydrogen Energy 2008;33:7580–91.
[15] Hu E, Huang Z, He J, Miao H. Experimental and numerical study on lean premixed methane–hydrogen–air flames at elevated pressures and temperatures. Int J Hydrogen Energy 2009;34:6951–60.
[16] Huang Z, Liu B, Zeng K, Huang Y, Jiang D, Wang X, et al. Combustion characteristics and heat release analysis of a spark-ignited engine fueled with natural gas–hydrogen blends. Energy Fuels 2007;21:2594–9.
[17] Huang Z, Liu B, Zeng K, Huang Y, Jiang D, Wang X, et al. Experimental study on engine performance and emissions for an engine fueled with natural gas–hydrogen mixtures. Energy Fuels 2006;20:2131–6.
[18] Hu E, Huang Z, He J, Jin C, Zheng J. Experimental and numerical study on laminar burning characteristics of premixed methane–hydrogen–air flames. Int J Hydrogen Energy 2009;34:4876–88.
[19] Hu E, Huang Z, Liu B, Zheng J, Gu X, Huang B. Experimental investigation on performance and emissions of a spark-ignition engine fuelled with natural gas–hydrogen blends combined with EGR. Int J Hydrogen Energy 2009;34:528–39.
[20] Hu E, Huang Z, Liu B, Zheng J, Gu X. Experimental study on combustion characteristics of a spark-ignition engine fueled with natural gas–hydrogen blends combining with EGR. Int J Hydrogen Energy 2009;34:1035–44.
[21] Huang B, Hu E, Huang Z, Zheng J, Liu B, Jiang D. Cycle-by-cycle variations in a spark ignition engine fueled with natural gas–hydrogen blends combined with EGR. Int J Hydrogen Energy 2009;34:8405–14.
[22] Ma F, Ding S, Wang Y, Wang Y, Wang J, Zhao S. Study on combustion behaviors and cycle-by-cycle variations in a turbocharged lean burn natural gas S.I. engine with hydrogen enrichment. Int J Hydrogen Energy 2008;33:7245–55.
[23] Reyes M, Melgar A, Pérez A, Giménez B. Study of the cycle-to-cycle variations of an internal combustion engine fuelled with natural gas/hydrogen blends from the diagnosis of combustion pressure. Int J Hydrogen Energy 2013;38:15477–87.
[24] Sen AK, Ash SK, Huang B, Huang Z. Effect of exhaust gas recirculation on the cycle-to-cycle variations in a natural gas spark ignition engine. Appl Therm Eng 2011;31:2247–53.
[25] Sun B-G, Zhang D-S, Liu F-S. Cycle variations in a hydrogen internal combustion engine. Int J Hydrogen Energy 2013;38:3778–83.
[26] Wang J, Chen H, Liu B, Huang Z. Study of cycle-by-cycle variations of a spark ignition engine fueled with natural gas–hydrogen blends. Int J Hydrogen Energy 2008;33:4876–83.
[27] Tinaut FV, Melgar A, Giménez B, Reyes M. Prediction of performance and emissions of an engine fuelled with natural gas/hydrogen blends. Int J Hydrogen Energy 2011;36:947–56.
[28] Horrillo A. Utilization of multi-zone models for the prediction of the pollutant emissions in the exhaust process in spark ignition engines. University of Valladolid; 1998.
[29] Lapuerta M, Armas O, Hernández JJ. Diagnosis of DI diesel combustion from in-cylinder pressure signal by estimation of mean thermodynamic properties of the gas. Appl Therm Eng 1999;19:513–29.
[30] Rakopoulos CD, Michos CN, Giakoumis EG. Availability analysis of a syngas fueled spark ignition engine using a multi-zone combustion model. Energy 2008;33:1378–98.
[31] Holland JH. Adaptation in natural and artificial systems an introductory analysis with applications to biology, control, and artificial intelligence.
[32] Gosselin L, Tye-Gingras M, Mathieu-Potvin F. Review of utilization of genetic algorithms in heat transfer problems. Int J Heat Mass Transf 2009;52:2169–88.
[33] Hernández JJ, Ballesteros R, Sanz-Argent J. Reduction of kinetic mechanisms for fuel oxidation through genetic algorithms. Math Comput Model 2010;52:1185–93.
[34] Tinaut F, Melgar A, Horrillo A. Utilization of a quasi-dimensional model for predicting pollutant emissions in SI engines. SAE Technical Paper. 1999. 1999-01-0223.
[35] Tinaut FV, Melgar A, Giménez B, Reyes M. Characterization of the combustion of biomass producer gas in a constant volume combustion bomb. Fuel 2010;89:724–31.
[36] Woschni G. A universally applicable equation for the instantaneous heat transfer coefficient in the internal combustion engine society of automotive engineers. SAE Technical Paper. 1967. SAE 670931.
[37] Reyes M, Tinaut FV, Giménez B, Pérez A. Characterization of cycle-to-cycle variations in a natural gas spark ignition engine. Fuel 2015;140:752–61.